Nanoparticle dispersion in superfluid helium

David P. Meichle and Daniel P. Lathrop
Department of Physics, Institute for Research in Electronics and Applied Physics, and Center for Nanophysics and Advanced Materials, University of Maryland, College Park, Maryland 20742, USA

Cryogenic fluid flows including liquid nitrogen and superfluid helium are a rich environment for novel scientific discovery. Flows can be measured optically and dynamically when faithful tracer particles are dispersed in the liquid. We present a reliable technique for dispersing commercially available fluorescent nanoparticles into cryogenic fluids using ultrasound. Five types of fluorescent nanoparticles ranging in size from 5 nm to 1 μm were imaged in liquid nitrogen and superfluid helium, and were tracked at frame rates up to 100 Hz. © *2014 AIP Publishing LLC.*
[http://dx.doi.org/10.1063/1.4886811]

I. INTRODUCTION

A. Background

Cryogenic fluids have interesting and unique dynamics. Experimental techniques to directly observe their flows open rich new opportunities for scientific exploration. Liquid nitrogen has a very low kinematic viscosity and is useful for study of fluid flows in parameter space unpractical with conventional liquids such as air or water.[1] Furthermore, liquid helium becomes a quantum fluid when cooled below the lambda transition temperature of 2.172 K. The superfluid state of liquid helium exhibits quantized vortices where vorticity is confined to line-like topological defects. Superfluid helium is also interesting by analogy to a wide range of systems including classical fluids, Bose-Einstein condensates, superconductors, and liquid crystals.

B. Frozen particles

The pioneering work of Bewley *et al.*[2,3] provided a method to produce micron-sized frozen (e.g., hydrogen ice) tracer particles in cryogenic liquids allowing for direct, optical measurements of liquid nitrogen and superfluid helium flows. Some fraction of the frozen ice particles become trapped on the quantized vortices in superfluid helium by a Bernoulli pressure gradient, enabling direct study of the vortex dynamics. This technique allowed for the experimental characterization of vortex reconnection[4–6] predicted by Feynman in 1955.[7] The two-fluid model of Landau was directly confirmed and the highly non-Gaussian velocity statistics of quantum turbulence were measured in a thermal counterflow.[4] Frozen particle accelerations have also been measured in a thermal counterflow.[8,9] Recently, the first direct observations of Kelvin waves, helical deformations of a vortex core, were observed on a quantized vortex following reconnection.[10] Frozen hydrogen particles have also been used to measure the flow of superfluid helium around a cylinder.[11]

C. Nanoparticle dispersion

While the frozen seed gas technique for creating particles has been scientifically fruitful, there is a need for a more reli-able method for creating tracer particles in cryogenic fluids, as well as the capability to use fluorescent particles. Very bright fluorescent nanoparticles of a wide range of sizes, emission and absorption wavelengths, and materials are readily available commercially as they are common in scientific biological, pharmaceutical, and medical microscopy applications.

We present here a simple and effective method for loading and dispersing commercially available fluorescent nanoparticles into cryogenic fluids using ultrasound. The technique may be used for particle sizes ranging from 100 μm down to several nanometers. This technique has also successfully dispersed nanoparticles directly into the superfluid state of liquid helium, something which is challenging with frozen particles.[3]

Additionally, the vortices in superfluid helium have been shown to create nanowires from gold nanoparticles.[12,13] This apparatus has successfully dispersed gold nanoparticles into the superfluid state of helium and offers an alternative method from laser ablation to disperse gold nanoparticles as in Ref. 13.

II. APPARATUS

A. Description

A schematic of the nanoparticle dispersal apparatus is shown in Figure 1, and it is shown attached to a typical optical-access cryostat in Figure 2. An ultrasound transducer is attached to an aluminum cone using metal epoxy. The narrow end of the cone is threaded to receive a quarter-inch thin-walled (.025 or .050 cm thick) stainless steel tube compatible with standard commercial cryostat vacuum feedthroughs, such as the Swagelock Ultratorr fittings. A stainless steel rod is threaded on one end, and the other is turned down to fit tightly inside the tube and silver-soldered inside. The ultrasound transducer is electrically driven with 1.5 kV signal at 45 kHz, with a transducer power of 500 W, only a tiny fraction of which is mechanically transmitted to the cryogen. Both the ultrasound transducer and drive electronics were taken from a commercially available bench-top ultrasound cleaner (McMaster-Carr #32695K38). A copper wire is wound and soldered to the tube end to increase the surface area, which
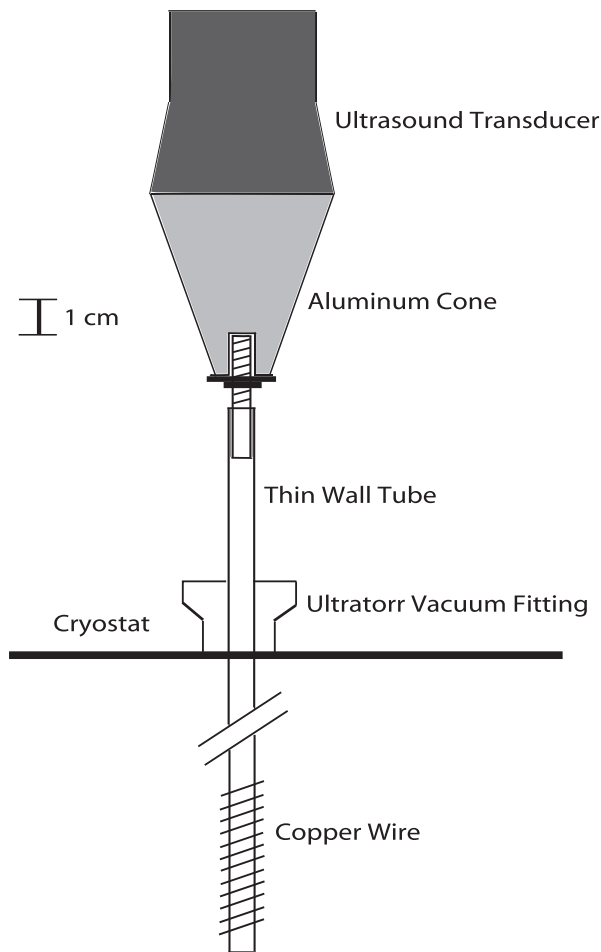
FIG. 1. Detailed schematic of a particle dispersal apparatus. An ultrasound transducer is attached to an aluminum cone which receives a thin-walled stainless steel tube compatible with standard vacuum port feedthrough. A spiral of copper wire is silver soldered to the bottom of the thin-walled tube. Nanoparticles in a high vapor pressure solvent are painted onto the bottom of the tube, and the solvent is evaporated at room temperature. After the sample section is cooled and filled with a cryogenic liquid, activating the transducer for less than 1 s disperses particles into the sample volume.

serves both to increase the number of nanoparticles which can be loaded and assist in applying the nanoparticle solution, described in the preparation steps below.

B. Experimental procedure

To prepare a sample, the desired quantity of nanoparticles are dissolved into a high vapor pressure solvent such as iso-propyl alcohol. Acetone should not be used as it was found to destroy the nanoparticles. Applying the solvent-nanoparticle solution to the bottom of the tube using a syringe leaves the nanoparticles coated on the tube after the solvent evaporates at room temperature. Acceptable and repeatable particle densities for a 350 ml liquid helium volume were obtained by mixing between 10 and 200 μl of the stock 20 nm and 100 nm fluorosphere 2% aqueous solution into 1 ml of isopropol alcohol. An initial loading of 200 μl of stock solution produced particle concentrations of order 20 particles per mm^3.

Slowly coating the bottom of the tube over about 20 min in several passes allows the excess solvent to evapo-
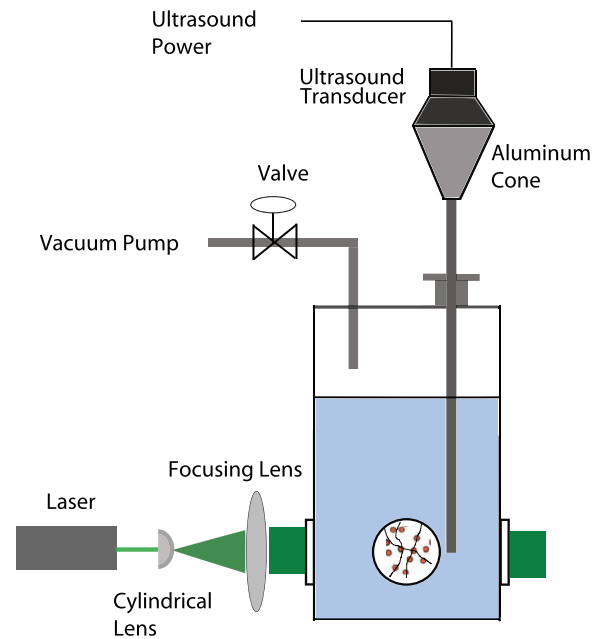

FIG. 2. The particle dispersal apparatus shown connected to an optical-access cryostat. A laser illuminates the cryogenic liquid sample section, in which fluorescent nanoparticles are dispersed allowing for flow visualization.

rate without dripping off the tube. The tube is then inserted into the cryostat and the transducer is fastened onto the tube outside the cryostat. After these preparation steps, one proceeds to load the cryogenic liquid. Once the end of the tube is submerged in the cryogenic liquid, activating the ultra-sound transducer for less than 1 s is sufficient to disperse the nanoparticles into the sample volume.

Repeated sonications are effective in both releasing more particles and stirring settled particles into the flow. As needed, additional short sonications will redistribute particles into the flow, counteracting the slow decrease in particle concentration due to sinking or adsorbing onto the sides of the container. In both liquid nitrogen and superfluid helium, it was possible to take movies for several hours with repeated short sonications (even below the lambda transition) every 5 to 10 min. When sonicating to redisperse particles, disturbances to the flow can be minimized by attenuating the ultrasound power by inserting a 10 kΩ high-voltage resistor in parallel with the transducer. Without attenuating the power, short sonications lasting about a quarter of a second were found to raise temperature of the helium sample section of order 10 mK, which we estimate corresponds to a heat input of order 5 J.

III. RESULTS

Commercially available semiconductor quantum dots, surface-plasmon resonant gold nanorods, and three sizes of polystyrene plastic beads loaded with fluorescent dyes were tested and successfully imaged in both liquid nitrogen and liquid helium. Table I lists details about the particles used. A 40 mW 532 nm laser illuminates a thin 10 mm × 10 mm × 175 μm volume through the cryostat windows. Fluorescent light from the particles is passed through a 532 nm notch filter and collected by a 105 mm Nikkor macro-lens with a numerical aperture of about 10°. Movies are recorded with

TABLE I. Details of all particle types successfully dispersed in both liquid helium and nitrogen.

Particle type	Manufacturer	Part number	Shipped form	Size (nm)	Excitation and Emission(nm)
Quantum Dots	Ocean Nanotech	QSP600	Powder	5	532/602
Gold nanorods	Nanopartz	E16-532	Organic solvent	25×35	533/556
FluoroSpheres	Life Technologies	F8784	Aqueous	20	532/575
FluoroSpheres	Life Technologies	F8800	Aqueous	100	540/560
FluoroSpheres	Life Technologies	F8819	Aqueous	1000	535/575

a Princeton Instruments ProEM cooled-CCD camera with 16 μm × 16 μm square pixels.

Sample particle trajectories of 20 nm Life Technologies fluorospheres in liquid helium at a mean temperature of 1.840 K are shown in Figure 3. Each dot represents a nanoparticle location separated by the 30 ms exposure time. These particle locations are assembled into tracks using a standard particle tracking routine.[14]

Additionally, a low noise, high speed VGA CCD camera was successfully used to image 100 nm Life Technologies fluorospheres in liquid nitrogen with a 10 msec exposure and the same optical configuration (ThorLabs part# 340M-GE).

Considering the size and brightness of the particles, as well as the toxicity and special handling required for gold nanoparticles and CdSe, the authors found the 20 nm and 100 nm Life Technologies fluorospheres to be optimal for superfluid helium experiments. Experimenters should develop safe handling procedures for all nanoparticles and the high voltage Ultrasound electronics.

A. Particle vortex interactions

We define the following dimensionless parameters: $\lambda = a/\zeta$ and $\sigma = s/\zeta$, where ζ is the vortex core size, s is the particle's distance from the vortex center, and a is the particle radius. The core size, near our working temperature of ≈1.7 K is $\zeta = \hbar/\sqrt{2m\mu} \approx 1$ Å, where $\hbar$ is the reduced Planck's constant, m is the mass of a helium atom, and μ is the temperature-dependent chemical potential.[18]

The force attracting the nanoparticle to the vortex core is assumed to be the force associated with the gradient of

the Bernoulli pressure.[3, 15, 16, 19] The Bernoulli pressure outside the vortex core is $P = \rho_s \kappa^2 / 8\pi^2 s^2$, where ρ_s is the superfluid density, κ is the quantum of circulation, and s is the radial distance away from the vortex center.

The force acting on the particle is given by the integral over the particle of the gradient of the pressure, or, equivalently, the surface integral of the pressure times the (negative) surface normal component,

$$\mathbf{F}_{\text{trap}} = -\int \nabla P \, \mathrm{d}^3\mathrm{V} = -\int_{\mathrm{dA}} P\hat{\mathbf{n}} \, \mathrm{d}^2\mathrm{A}. \qquad (1)$$

The integration domain dA is over the surface of the particle.

The magnitude of $\mathbf{F}_{\text{trap}}$ is approximated in the far field, for distances far from the vortex core where the gradient of the pressure and the superfluid density are nearly constant. The familiar far field approximation[3, 15, 16, 19] for the magnitude of the attractive force is given by the product of the volume of the particle and the far field pressure force:

$$F_{\text{trap}} \approx -\left(\frac{4}{3}\pi a^3\right)\frac{\rho_s \kappa^2}{8\pi^2}\nabla(1/s^2) = \left(\frac{\lambda}{\sigma}\right)^3 \frac{\rho_s \kappa^2}{3\pi}. \qquad (2)$$

However, near the vortex core this approximation is not valid as the vortex may curve[15] and the superfluid density is not constant.[18] We expect the trapping force to be a function of the two dimensionless parameters λ and σ defined above. The trapping force should take the form

$$F_{\text{trap}} = -\rho_s \kappa^2 f_m(\sigma, \lambda), \qquad (3)$$

where ρ_s is the temperature-dependent background superfluid density, and f_m dimensionless scalar function. The function f_m will incorporate the non-uniform superfluid density effects, which are dependent on σ near the vortex core.

We expect the maximal trapping force to occur when the particle is displaced one radius from the vortex center, i.e., where $\sigma/\lambda \rightarrow 1$. If $f_m(\lambda) \propto \lambda^\alpha$, for $\alpha \leq 1$, then the maximal trapping force is increased with smaller particle radii. Indeed, Chagovets and Sciver[19] give $f_m(\lambda) = \log(\lambda)$.

In addition to the Bernoulli pressure gradient attracting the particles to the vortex core, we assume that the normal fluid exerts a viscous force (Stokes drag) on the particles.[3, 15, 16, 19] The force from Stokes drag is given by

$$\mathbf{F}_{\text{stokes}} = 6\pi a\nu\rho_n(\mathbf{v_n} - \mathbf{v_p}). \qquad (4)$$

Here a is the nanoparticle's radius, ρ_n is the normal fluid density, ν is the kinematic viscosity, and $(\mathbf{v_n} - \mathbf{v_p})$ is the velocity difference between the normal fluid and the particle.

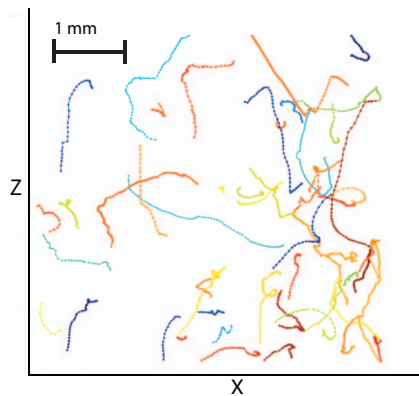The particle may be dislodged from the vortex when viscous drag from the normal fluid overcomes the attractive

FIG. 3. Trajectories of 20 nm fluorospheres at 1.840 K in superfluid helium. Each point is separated by 30 ms. Individual particle trajectories are assembled with a particle tracking package.[14] Sudden accelerations and oscillatory motions, likely from vortex core trapping and un-trapping events as well as vortex reconnections are present.

Bernoulli pressure gradient. The maximal velocity that a particle can be dragged through the normal fluid while remaining trapped on the vortex core is found by equating the trapping force and Stokes drag and solving for the velocity difference. The maximum velocity should scale as

$$v_m \propto \frac{\rho_s}{\rho_n} \frac{\kappa^2}{\nu} \frac{f_m(\lambda, \sigma)}{a}. \tag{5}$$

This maximum velocity is increased for smaller particles because both Stokes drag is reduced and the trapping force is increased. This could allow for studies of vortex dynamics at higher speeds, which may enable measurements of great scientific interest as the vortex velocities diverge (limited by the speed of sound) in individual vortex reconnections.

B. Comparison to frozen particles

Figure 4(a) shows 20 nm Life fluorospheres dispersed in superfluid helium at 2.094 K. For comparison, a typical image of frozen particles used in the seminal experiments of Bewley and Paoletti is shown in Figure 4(b). The nanoparticles provide several optical advantages, including a more uniform size and brightness distribution, and better signal to noise as a result of their efficient fluorescence and the ability to filter out the excitation light with a 532 nm optical notch filter. Filtering allows the imaging optics to isolate the particle's fluorescent light, removing the excitation light and stray lab light. Filtering could allow for previously difficult optical configurations, where, for example, particles could be imaged flowing around structures in the liquid which would otherwise scatter too much light and saturate the camera.

The frozen particles in Figure 4(b) were illuminated with a 6 W argon continuous laser, whereas the nanoparticles in Figure 4(a) were illuminated with 40 mW from a diode laser. The nanoparticles are relatively brighter, requiring substantially less illumination light. This is important as higher laser powers heat the cryostat windows and generate a thermal counterflow which disturbs the flow.

Avoiding the injection of a seed gas prevents the formation of large nonuniform aggregates, which affect the helium and vortex dynamics, and can saturate the imaging system.

Since the trapping force is short range, it is important to consider what density of particles per volume is needed to decorate the vortices sufficiently to track their motions. We solve for a capture distance where the pressure field attracting the particle overcomes Stokes drag from the normal component by equating Stokes drag and the far-field attractive force, given by Eqs. (2) and (4) and then solving for s. This gives a capture distance s_c, given by

$$s_c = \left(\frac{a^2}{18\pi^2} \frac{\rho_s}{\rho_n} \frac{\kappa^2}{\nu} \right)^{1/3}. \tag{6}$$

For a 100 nm particle at 1.85 K and a normal fluid velocity of 5 μm/s, as was measured in Ref. 10, this capture distance is about 20 μm. Figure 5 shows this distance versus normal fluid velocity for three particle sizes. This capture distance is reduced for smaller particles, scaling as $a^{2/3}$, so we expect higher seeding densities (particles per volume)
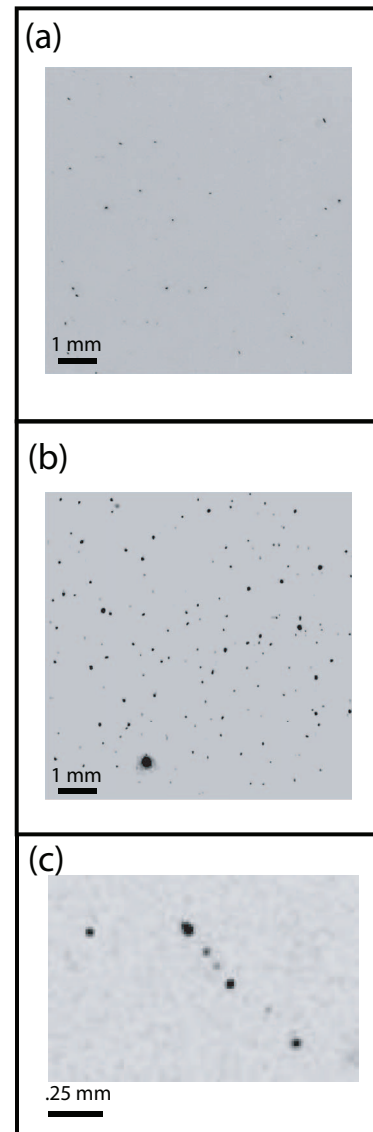

FIG. 4. (a) Contrast enhanced inverted sample image of 20 nm fluorospheres at 1.758 K in liquid helium, with a 30 ms exposure. (b) Typical frozen hydrogen particle image similar to Bewley[2] and Paoletti[4] with a 16 ms exposure. The frozen particle image was taken with a 6 W continuous-wave argon laser illuminating the particles, whereas the nanoparticle image was taken with a 40 mW 532 nm diode laser. The nanoparticle image shows a more uniform particle brightness distribution, filtering the excitation light significantly reduces the background light level, and there are no large frozen agglomerates which were often present in frozen particle movies. (c) A vortex segment decorated with 100 nm fluorospheres at 1.790 K in liquid helium with a 10 ms exposure, demonstrating that the nanoparticles can be trapped on the quantized vortex cores.

are required to decorate vortices than with frozen particles. Figure 5 shows the capture distance as a function of typical background normal fluid velocities for three particle sizes.

Sinking due to buoyancy is a small effect. A free fall velocity can be found by equating Stokes drag and the buoyancy force.[20] For a 100 nm polystyrene sphere, the terminal free fall speed is about 1 μm/s, and for a 20 nm sphere the free fall speed is about 50 nm/s; these free fall speeds are insignificant for current vortex dynamics studies.

We estimate the binding energy of a nanoparticle by computing the excluded superfluid kinetic energy, as in Parks and Donnelly[21] and Bewley and Vollmer.[17] For a 100 nm parti-
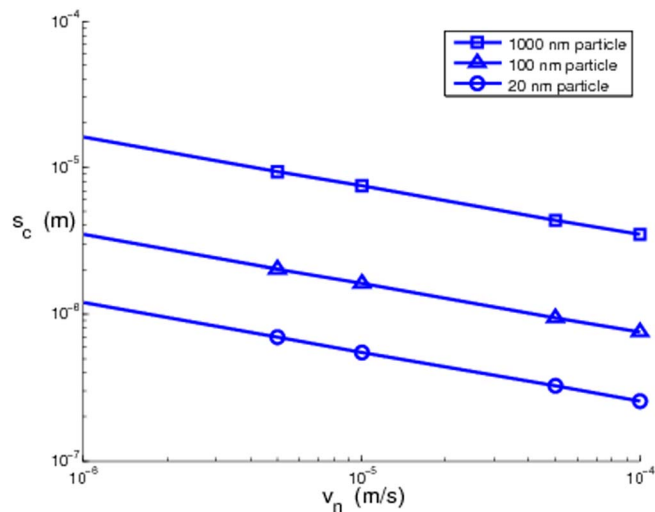
FIG. 5. Calculated capture distance s_c below which the trapping force becomes greater than Stokes drag from the normal fluid, as a function of the normal fluid velocity. Three different particle sizes are shown.

cle at 1.85 K, the binding energy is estimated to be about 5 $\times$ 10^{-20} J, which is 1.5×10^3 times $k_b T$, where k_b is Boltzmann's constant. Since the binding energy is many times $k_b T$, we expect particles to remain trapped and not removed due to purely thermal motions.

IV. CONCLUSIONS

Fluid flows are frequently measured optically by dispersing faithful tracer particles and observing their motions. However, creating and dispersing robust fluid tracer particles in cryogenic fluids has been notoriously difficult. Here, we have described the apparatus and procedures by which nanometer scale tracer particles can be reliably dispersed into cryogenic fluids and which can readily be applied in measurements with traditional liquid-helium-cooled cryostats. As commercial fluorescent nanoparticles have become widely available, this approach opens new possibilities in flow metrology, including the techniques of particle image velocimetry or particle tracking.

[1]E. Fonda, K. R. Sreenivasan, and D. P. Lathrop, "Liquid nitrogen in fluid dynamics: Visualization and velocimetry using frozen particles," Rev. Sci. Instrum. **83**(8), 085101 (2012).

[2]G. P. Bewley, D. P. Lathrop, and K. R. Sreenivasan, "Superfluid Helium: Visualization of quantized vortices," Nature **441**(7093), 588 (2006).

[3]G. P. Bewley, K. R. Sreenivasan, and D. P. Lathrop, "Particles for tracing turbulent liquid helium," Exp. Fluids **44**(6), 887–896 (2008).

[4]M. Paoletti, M. Fisher, K. Sreenivasan, and D. P. Lathrop, "Velocity statistics sistinguish quantum turbulence from classical turbulence," Phys. Rev. Lett. **101**(15), 154501 (2008).

[5]G. P. Bewley, M. S. Paoletti, K. R. Sreenivasan, and D. P. Lathrop, "Characterization of reconnecting vortices in superfluid helium," Proc. Natl. Acad. Sci. U.S.A. **105**(37), 13707–13710 (2008).

[6]M. S. Paoletti, M. E. Fisher, and D. P. Lathrop, "Reconnection dynamics for quantized vortices," Physica D **239**(14), 1367–1377 (2010).

[7]R. Feynman, *Progress in Low Temperature Physics*, edited by C. J. Gorter (North-Holland, Amsterdam, 1955), pp. 17–53.

[8]M. La Mantia, T. V. Chagovets, M. Rotter, and L. Skrbek, "Testing the performance of a cryogenic visualization system on thermal counterflow by using hydrogen and deuterium solid tracers," Rev. Sci. Instrum. **83**, 055109 (2012).

[9]M. La Mantia, D. Duda, M. Rotter, and L. Skrbek, "Lagrangian accelerations of particles in superfluid turbulence," J. Fluid Mech. **717**, R9 (2013).

[10]E. Fonda, D. P. Meichle, N. T. Ouellette, S. Hormoz, and D. P. Lathrop, "Direct observation of Kelvin waves excited by quantized vortex reconnection," Proc. Natl. Acad. Sci. U.S.A., **111**(Supplement 1) 4647–4652 (2014).

[11]T. V. Chagovets and S. W. Van Sciver, "Visualization of He II counterflow around a cylinder," Phys. Fluids **25**, 105104 (2013).

[12]P. Moroshkin, V. Lebedev, B. Grobety, C. Neururer, E. B. Gordon, and A. Weis, "Nanowire formation by gold nano-fragment coalescence on quantized vortices in He II," Europhys. Lett. **90**(3), 34002 (2010).

[13]V. Lebedev, P. Moroshkin, B. Grobety, E. Gordon, and A. Weis, "Formation of metallic manowires by laser ablation in liquid helium," J. Low Temp. Phys. **165**, 166 (2011).

[14]D. Grier, J. C. Crocker, and E. R. Weeks, See http://www.physics.emory. edu/weeks/idl/index.html for particle tracking code.

[15]Y. Mineda, M. Tsubota, Y. A. Sergeev, C. F. Barenghi, and W. F. Vinen, "Velocity distributions of tracer particles in thermal counterflow in superfluid ^{4}He," Phys. Rev. B **87**, 174508 (2013).

[16]Y. A. Sergeev and C. F. Barenghi, "Particles-vortex interactions and flow visualization in ^{4}He," J. Low Temp. Phys. **157**, 429–475 (2009).

[17]G. P. Bewley and J. Vollmer, "The journey of hydrogen to quantized vortex cores," Phys. Scr. **T155**, 014055 (2013).

[18]D. P. Meichle, C. Rorai, M. E. Fisher, and D. P. Lathrop, "Quantized vortex reconnection: Fixed points and initial conditions," Phys. Rev. B **86**, 014509 (2012).

[19]T. V. Chagovets and S. W. Van Sciver, "A study of thermal counterflow using particle tracking velocimetry," Phys. Fluids **23**, 107102 (2011).

[20]G. P. Bewley, Ph.D. thesis, Yale University, 2006.

[21]P. E. Parks and R. J. Donnelly, "Radii or positive and negative ions in helium II," Phys. Rev. Lett. **16**(2), 45 (1966).